

A Discrete Flux Scheme for Aerodynamic and Hydrodynamic Flows

S. C. Fu^{1,*}, R. M. C. So^{1,2} and W. W. F. Leung^{1,3}

¹ Mechanical Engineering Department, Hong Kong Polytechnic University, Hung Hom, Kowloon, Hong Kong.

² School of Mechanical Engineering, Purdue University, West Lafayette, IN 47907-2088, USA.

³ Research Institute of Innovative Products & Technologies, Hong Kong Polytechnic University, Hung Hom, Kowloon, Hong Kong.

Received 31 October 2009; Accepted (in revised version) 24 November 2010

Available online 28 January 2011

Abstract. The objective of this paper is to seek an alternative to the numerical simulation of the Navier-Stokes equations by a method similar to solving the BGK-type modeled lattice Boltzmann equation. The proposed method is valid for both gas and liquid flows. A discrete flux scheme (DFS) is used to derive the governing equations for two distribution functions; one for mass and another for thermal energy. These equations are derived by considering an infinitesimally small control volume with a velocity lattice representation for the distribution functions. The zero-order moment equation of the mass distribution function is used to recover the continuity equation, while the first-order moment equation recovers the linear momentum equation. The recovered equations are correct to the first order of the Knudsen number (Kn); thus, satisfying the continuum assumption. Similarly, the zero-order moment equation of the thermal energy distribution function is used to recover the thermal energy equation. For aerodynamic flows, it is shown that the finite difference solution of the DFS is equivalent to solving the lattice Boltzmann equation (LBE) with a BGK-type model and a specified equation of state. Thus formulated, the DFS can be used to simulate a variety of aerodynamic and hydrodynamic flows. Examples of classical aeroacoustics, compressible flow with shocks, incompressible isothermal and non-isothermal Couette flows, stratified flow in a cavity, and double diffusive flow inside a rectangle are used to demonstrate the validity and extent of the DFS. Very good to excellent agreement with known analytical and/or numerical solutions is obtained; thus lending evidence to the DFS approach as an alternative to solving the Navier-Stokes equations for fluid flow simulations.

AMS subject classifications: 76M25, 76D05

Key words: Aerodynamics, hydrodynamics, lattice Boltzmann equation.

*Corresponding author. *Email addresses:* mm.scfu@polyu.edu.hk (S. C. Fu), mmmcs@polyu.edu.hk (R. M. C. So), mmwleung@polyu.edu.hk (W. W. F. Leung)

1 Introduction

The Bhatnagar-Gross-Krook (BGK)-type [1] modeled lattice Boltzmann equation proves to be a viable alternative to the Navier-Stokes (NS) equations for fluid flow simulations and the associated transport phenomena [2–5]. The original Boltzmann equation was derived by stipulating the assumption of ideal gas and the neglect of the intermolecular interaction. The BGK-type modeled Boltzmann equation (MBE) is a scalar equation governing the transport of a particle distribution function f . In order to solve this equation, a conventional approach is to assume a velocity lattice model, thus giving rise to the lattice Boltzmann method (LBM). The scalar equation for f is then transformed into N number of lattice equations; therefore, the process of solving the vector and tensor NS equations is reduced to using LBM to solve the set of scalar equations. With the development of more and more accurate numerical methods, the BGK-type modeled lattice Boltzmann equation (LBE) found success not only in aerodynamic flows but also in the simulations of thermodynamic flows [6,7]. Extension to one-step aeroacoustics simulations [8,9], to acoustic scattering simulations [10,11], and to shock capturing and shock structure simulations [12,13] has also been successfully demonstrated. The simulations are in good agreement with analytical and other known numerical results.

Most of these studies were focused on gas flows where an ideal gas equation of state was specified. For non-ideal gas and fluid flows with multiple phases and components, the appropriateness of the traditional LBM is doubtful. Since the mean-field approximation is widely used in liquid theory [14], the same approach has been extended to treat non-ideal gas flows, fluid flows with phase transitions and binary immiscible fluids [15–18]. These studies were mainly focused on the recovery of the NS equations. A recent theoretical study to represent hydrodynamic systems through a systematic discretization of the Boltzmann kinetic equation has been attempted [19]; it manages to show an alternative way to recover fluid dynamic equations, from the NS equations to Burnett fluids and beyond. As a result, a systematic approach to derive the NS equations based on the kinetic level of representation is available; the approach is not subject to the assumption of an ideal gas law and the neglect of intermolecular interaction. In principle, this latest approach can be used to treat incompressible flow of liquids, such as the double diffusive phenomenon found in ocean layers [20–22]. However, the application of LBM to this branch of fluid dynamics is still lacking. The present work attempts to examine the validity and extent of the application of LBM-type technique or its variant to oceanography.

Using the Hermite expansion approach, Shan et al. [19] showed that fluid flows can be systematically approximated by constructing higher-order LBE models. Instead of adopting this approach to derive a LBE that could recover the NS equations exactly for incompressible (with constant density assumed) and compressible fluid flows, an alternative approach is sought in the present study. Due to the simplicity of the BGK-type modeled LBE, its extension to hydrodynamic problems is both appropriate and desirable, if the assumption of an ideal gas law can be lifted. The focus is on the recovery of

the continuum NS equations. If incompressible flows were to be simulated exactly, the assumption of a very small Mach number ($M \ll 1$) [23] should be avoided. This is because the $M \ll 1$ assumption is not equivalent to the necessary and sufficient condition for an incompressible flow, which is characterized by zero total rate of change of density (ρ) in the whole flow field [24]. A way to impose this zero total rate of change of ρ condition in the solution of the BGK-type modeled LBE has been put forward in [25].

The present objective, therefore, is to seek an alternative way to derive the BGK-type modeled LBE that can recover the continuum NS equations fully and is equally valid for gas and liquid flows. This BGK-type modeled LBE is derived based on a discrete flux scheme (DFS). A two equation formulation much like that proposed in [26,27] is adopted. These two equations are derived heuristically using the control volume approach, and they are very similar to the BGK-type modeled LBE. One equation governs the transport of \tilde{f} , a distribution function used to represent an intrinsic flow property, such as the fluid density, at an infinitesimally small control volume. Another equation governs the transport of \tilde{g} , which is proposed to represent the distribution function of the total thermal energy of the infinitesimally small control volume of moving fluid. Hereafter, a symbol with a tilde is used to represent the dimensional property, while a symbol without a tilde is used to represent its corresponding dimensionless property.

In anticipation of the fact that the velocity lattice technique is used to solve the \tilde{f} and \tilde{g} equations, only the derivation of the equations for \tilde{f}_α and \tilde{g}_α (the lattice counterpart of \tilde{f} and \tilde{g} , respectively) is presented together with the recovery of the full set of NS equations from the transport equations for \tilde{f}_α and \tilde{g}_α . Here α is an index used to denote the velocity lattice. Note it is not necessary to invoke an equation of state in the recovery of the NS equations. The next step is to establish equivalency of this two-equation approach to the single-equation formulation for compressible gas flows [13]. If the validity and extent of the NS equations were to be fully replicated in the equivalent BGK-type modeled LBE, the ability of the present approach to simulate incompressible flows needs to be established. This can be accomplished by treating incompressible, non-isothermal flows with $\rho = \text{constant}$ instead of assuming $M \ll 1$ as proposed in [23]. Finally, it is shown that the present approach can be extended to treat buoyant flows where double diffusion occurs. The overall formulation is given in detail, but only examples of shock structure simulation and buoyant flow calculation are discussed because other examples of incompressible, non-isothermal gas and/or liquid flows have been reported in [28].

2 Discrete flux scheme (DFS) as an alternative to the Navier-Stokes (NS) equations

It should be pointed out from the beginning that the DFS is a numerical scheme proposed for the solution of the NS equations. The governing equations for \tilde{f}_α and \tilde{g}_α are derived and their equivalency to the mass, momentum and energy transport equations is estab-

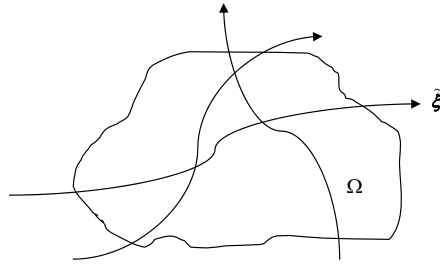


Figure 1: Pictorial representation of the control volume $\tilde{\Omega}$ in the flow field.

lished. In order to establish this equivalency, \tilde{f}_α has to satisfy certain constraints similar to those used to establish equivalency between the MBE and the NS equations. The function \tilde{g}_α also has to satisfy certain constraints if the thermal energy equation of the set of NS equations were to be recovered correctly. In the process, the set of vector and tensor NS equations are reduced to a finite number of scalar equations. Thus derived, the equations for \tilde{f}_α and \tilde{g}_α are of the convective-diffusive type and can be solved numerically using a splitting technique [29]. The extension of this approach to account for external body force effect is also presented. This is carried out with the aim to provide a general framework for any type of external body force, including buoyancy. The resulting equations are then used to treat problems such as double diffusion in ocean layers.

2.1 Discrete flux representation of the mass and momentum equation

Consider a control volume Ω of continuum fluid with a finite volume $\tilde{\Omega}$ and an arbitrary shape fixed in space (see Fig. 1). The center of Ω is located at coordinates (x, y, z) , and the fluid is assumed to move through Ω . The corresponding mass \tilde{m} of the fluid inside Ω is assumed to move at velocity $\tilde{\xi}$, while $\tilde{\rho}$ at (x, y, z) can be defined by an averaging process, such that,

$$\tilde{\rho}(x, y, z) = \frac{1}{\tilde{\Omega}} \int_{\tilde{\Omega}} \tilde{m} d\tilde{\xi}, \quad (2.1)$$

while the velocity $\tilde{\mathbf{u}}$ of the fluid at (x, y, z) is also defined by a mass-averaging process, i.e.,

$$\tilde{\mathbf{u}}(x, y, z) = \frac{\frac{1}{\tilde{\Omega}} \int_{\tilde{\Omega}} \tilde{m} \tilde{\xi} d\tilde{\xi}}{\frac{1}{\tilde{\Omega}} \int_{\tilde{\Omega}} \tilde{m} d\tilde{\xi}}. \quad (2.2)$$

In parallel with the derivation of the conventional LBE, a discrete representation is proposed. Consequently, it is assumed that there are only a finite number of velocities $\tilde{\xi}_\alpha$ for consideration. An intrinsic property \tilde{f}_α relating to the density of the fluid corresponding to a group of fluid masses moving with the same velocity $\tilde{\xi}_\alpha$ is defined so that the

following can be obtained

$$\tilde{\rho} = \sum_{\alpha} \tilde{f}_{\alpha}, \quad (2.3a)$$

$$\tilde{\rho} \tilde{\mathbf{u}} = \sum_{\alpha} \tilde{f}_{\alpha} \tilde{\boldsymbol{\zeta}}_{\alpha}, \quad (2.3b)$$

where $\tilde{f}_{\alpha} = W_{\alpha} \tilde{m}_{\alpha} / \tilde{\Omega}$ is a discrete form of representing the distribution function \tilde{f} , and \tilde{m}_{α} is a discrete form of representing the mass \tilde{m} . After invoking the discrete flux model, the number of velocity $\tilde{\boldsymbol{\zeta}}_{\alpha}$ varies from essentially an infinite number to a finite number. In view of this, it is convenient to introduce a weighting function W_{α} to account for the summation, which acts like a numerical integration. The weighting function W_{α} may be negative, hence, \tilde{f}_{α} may also be negative. However, the sum of \tilde{f}_{α} should always be positive. Due to the discrete choice of the velocities $\tilde{\boldsymbol{\zeta}}_{\alpha}$, the flux of the flow properties is represented in a discrete manner and hence the name "discrete flux" is used.

Since \tilde{f}_{α} is corresponding to a group of masses of fluid moving with the same velocity $\tilde{\boldsymbol{\zeta}}_{\alpha}$, the total rate of change of \tilde{f}_{α} in Ω is $(\partial \tilde{f}_{\alpha} / \partial \tilde{t} + \tilde{\boldsymbol{\zeta}}_{\alpha} \cdot \nabla \tilde{f}_{\alpha})$, which is not necessarily zero, because the velocity of these masses of fluid will change as a result of collision and/or the effect of intermolecular forces between fluid molecules. If it is assumed that there exists a "local equilibrium" state for \tilde{f}_{α} , denoted as \tilde{f}_{α}^{eq} , such that when \tilde{f}_{α} reaches its local equilibrium state, its rate of change vanishes. When the masses of fluid inside Ω are not in their local equilibrium states, it is argued that they will rearrange their velocities to approach \tilde{f}_{α}^{eq} as a result of collision and/or the effect of intermolecular forces as mentioned before. The time required for the rearrangement can be designated as the "relaxation time", $\tilde{\tau}$, which is substantially smaller than the flow characteristic time \tilde{t}_0 , much like that proposed in the BGK model for the conventional LBE. Following the argument of the BGK model, it is further assumed that $(\partial \tilde{f}_{\alpha} / \partial \tilde{t} + \tilde{\boldsymbol{\zeta}}_{\alpha} \cdot \nabla \tilde{f}_{\alpha})$ is proportional to the difference between \tilde{f}_{α} and \tilde{f}_{α}^{eq} , or

$$\frac{\partial \tilde{f}_{\alpha}}{\partial \tilde{t}} + \tilde{\boldsymbol{\zeta}}_{\alpha} \cdot \nabla \tilde{f}_{\alpha} = -\frac{\tilde{f}_{\alpha} - \tilde{f}_{\alpha}^{eq}}{\tilde{\tau}}. \quad (2.4)$$

After normalizing \tilde{f}_{α} by a characteristic density $\tilde{\rho}_0$, $\tilde{\boldsymbol{\zeta}}_{\alpha}$ by \tilde{u}_0 , time, including $\tilde{\tau}$, by \tilde{t}_0 , and space by \tilde{l}_0 , respectively, the dimensionless form of Eq. (2.4) is given by

$$\frac{\partial f_{\alpha}}{\partial t} + \boldsymbol{\zeta}_{\alpha} \cdot \nabla f_{\alpha} = -\frac{f_{\alpha} - f_{\alpha}^{eq}}{\varepsilon \tau}, \quad (2.5)$$

where ε is a small parameter that can be interpreted as similar to the Knudsen number (Kn). It will be shown later that this interpretation is consistent with the continuum assumption.

If, in addition, it is assumed that the deviation of f_{α} from f_{α}^{eq} is very small, then f_{α} can be written in terms of f_{α}^{eq} and a small non-equilibrium component f_{α}^{neq} , such that

$$f_{\alpha} = f_{\alpha}^{eq} + \varepsilon f_{\alpha}^{neq}. \quad (2.6)$$

Thus defined, f_α^{eq} can be determined if certain constraints are satisfied. These constraints are put forward with the objective that the f_α^{eq} thus obtained can be used in Eq. (2.5) to recover the mass and momentum equation in the set of NS equations. These constraints are

$$\sum_\alpha f_\alpha^{eq} = \rho, \quad (2.7a)$$

$$\sum_\alpha f_\alpha^{eq} (\xi_\alpha)_i = \rho u_i, \quad (2.7b)$$

$$\sum_\alpha f_\alpha^{eq} (\xi_\alpha)_i (\xi_\alpha)_j = \rho u_i u_j + p \delta_{ij} - \tau_{ij}. \quad (2.7c)$$

From this point on, the indices i and j are also used to denote vectors and second-order tensors. The first two constraints are similar to the mass and linear momentum definitions given in Eqs. (2.3a), (2.3b) and those found in the evaluation of an equilibrium particle distribution function of the LBM [3]. The third constraint is proposed to ensure the recovery of the momentum equation in the NS equations. Therefore, τ_{ij} , which is the dimensionless viscous stress tensor, is defined as

$$\tau_{ij} = -\frac{M_\infty}{Re_\infty} \left\{ 2\mu \left(S_{ij} - \frac{1}{3} \delta_{ij} S_{kk} \right) \right\}, \quad (2.8)$$

where the strain tensor S_{ij} is given by $S_{ij} = (\partial u_i / \partial x_j + \partial u_j / \partial x_i) / 2$, μ is the first coefficient of viscosity and is made dimensionless by a reference μ_0 , M_∞ is a reference Mach number and Re_∞ is a reference Reynolds number. Multiplying Eq. (2.5) with respect to $\{1, (\xi_\alpha)_i\}^T$, taking summation over α , and using the expressions given in Eqs. (2.7a)-(2.7c), the exact mass conservation equation and the momentum equation accurate to order ε of the NS equations set are obtained; they can be written as

$$\frac{\partial \rho}{\partial t} + \sum_j \frac{\partial \rho u_j}{\partial x_j} = \frac{D\rho}{Dt} + \rho \sum_j \frac{\partial u_j}{\partial x_j} = 0, \quad (2.9a)$$

$$\frac{\partial (\rho u_i)}{\partial t} + \sum_j \frac{\partial}{\partial x_j} (\rho u_i u_j + p \delta_{ij} + \tau_{ij}) = \mathcal{O}(\varepsilon). \quad (2.9b)$$

It can be seen that if ε is interpreted as Kn , the correct NS equations for a continuum fluid are recovered.

2.2 Discrete flux representation of the energy equation

Similar to f_α , another flux distribution function, g_α , representing the total thermal energy e_t is introduced, such that

$$\rho e_t = \rho \left(e + \frac{1}{2} |\mathbf{u}|^2 \right) = \sum_i g_\alpha, \quad (2.10)$$

where e_t and e , and g_α have been normalized by \tilde{u}_0^2 and $\tilde{\rho}_0 \tilde{u}_0^2$, respectively, to make them dimensionless. Similar to the argument of f_α , although g_α is related to the total energy, its individual value can be negative due to the finite number of discrete velocities assumed. The equilibrium state of g_α is g_α^{eq} . Consequently, g_α can be written in terms of g_α^{eq} plus a non-equilibrium state g_α^{neq} , i.e.,

$$g_\alpha = g_\alpha^{eq} + \varepsilon g_\alpha^{neq}. \quad (2.11)$$

The equation that governs the transport of g_α can again be derived in a manner similar to that for f_α . The result is

$$\frac{\partial g_\alpha}{\partial t} + \xi_\alpha \cdot \nabla g_\alpha = -\frac{g_\alpha - g_\alpha^{eq}}{\varepsilon \tau}. \quad (2.12)$$

If the thermal energy equation in the NS equations were to be recovered correctly, g_α^{eq} has to satisfy the following constraints

$$\sum_\alpha g_\alpha^{eq} = \rho \left(e + \frac{1}{2} |\mathbf{u}|^2 \right), \quad (2.13a)$$

$$\sum_\alpha g_\alpha^{eq} (\xi_\alpha)_i = u_i \left(p + \rho e + \frac{1}{2} \rho |\mathbf{u}|^2 \right) + \sum_j u_j \tau_{ij} + q_i, \quad (2.13b)$$

where the heat flux vector q_i is given by

$$q_i = -\frac{\gamma M_\infty}{Re_\infty Pr_\infty} \left(\kappa \frac{\partial e}{\partial x_i} \right), \quad (2.14)$$

Pr_∞ is a reference Prandtl number, and κ is the fluid coefficient of thermal conductivity made dimensionless by a reference κ_0 . Eq. (2.13a) is similar to the definition of e_t given in Eq. (2.10), and Eq. (2.13b) simply ensures the recovery of the energy equation in the NS equations. Taking summation over α in Eq. (2.12), and using the expressions given in Eqs. (2.13a) and (2.13b), the thermal energy equation is recovered, i.e.,

$$\frac{\partial}{\partial t} \left(\rho e + \frac{1}{2} \rho |\mathbf{u}|^2 \right) + \sum_j \frac{\partial}{\partial x_j} \left[u_j \left(\rho e + \frac{1}{2} \rho |\mathbf{u}|^2 + p \right) + \sum_k u_k \tau_{jk} + q_j \right] = \mathcal{O}(\varepsilon). \quad (2.15)$$

From the above derivation, it is clear that solving Eqs. (2.5) and (2.12) is equivalent to solving the NS equations given by Eqs. (2.9a), (2.9b) and (2.15). For compressible gas flows, an equation of state is required to close the equation set; however, for incompressible flows of gas or liquid, no such requirement is necessary. Before proceeding to discuss the numerical methods used to solve Eqs. (2.5) and (2.12), an extension of this general approach to treat flows with external body forces is outlined below. The method proposed is general enough for any external body force, including that introduced by the implementation of the immersed boundary technique [30].

2.3 Extension of methodology to flow with external body force

The effect of an external body force, such as buoyancy in a stratified flow, can be easily accounted for in the present discrete flux formulation. In order to account for this effect, Eq. (2.5) can be modified to read

$$\frac{\partial f_\alpha}{\partial t} + \boldsymbol{\zeta}_\alpha \cdot \nabla f_\alpha + F_\alpha = -\frac{f_\alpha - f_\alpha^{eq}}{\varepsilon\tau}, \quad (2.16)$$

where F_α is the dimensionless rate of change of density of fluid elements moving with velocity $\boldsymbol{\zeta}_\alpha$ in the control volume Ω due to the applied force field. It has to fulfill the following constraints,

$$\sum_\alpha F_\alpha = 0, \quad (2.17a)$$

$$\sum_\alpha F_\alpha \boldsymbol{\zeta}_\alpha = \mathbf{F}_b, \quad (2.17b)$$

where \mathbf{F}_b is the dimensionless external body force applied to the flow field. The constraint given by Eq. (2.17a) implies that the body force does not affect the total mass inside Ω . In Eq. (2.17b), F_α multiplies by velocity $\boldsymbol{\zeta}_\alpha$ is the rate of change of momentum due to the external force field, thus it is the body force itself. Therefore, this approach can be used to recover the buoyant force in the NS equations written for stratified flow. This approach to account for the effect of external body forces can be easily generalized to treat boundary with arbitrary geometries. An example is the immersed boundary method [30] where the boundary shape can be represented by a balance of fluid forces acting on the boundary.

3 Relation between DFS and LBE

The mathematical framework and the concomitant physical meaning of the discrete flux scheme proposed as an alternative to solving the NS equations have been presented. The next step is to establish its relation to the lattice Boltzmann equation (LBE) derived based on the gas-kinetic approach. This can be accomplished by presenting the following cases separately and elaborating on the relation between the DFS approach and that of the LBE, and the numerical methods used to solve the specific cases. These are: Case A-compressible flow with an ideal gas law; Case B-incompressible isothermal and non-isothermal flow; and Case C-stratified flow. In the following, it is shown that the present two-distribution-function DFS formulation can be reduced to a single-distribution-function formulation of the conventional LBE for gas flows (Case A). If the flow is incompressible (whether isothermal or non-isothermal with decoupled energy equation), there is no need to specify a state equation in the simulation; however, conventional LBE is applicable provided a method is available for the determination of the pressure field. It should be noted that the same form of equations is solved by the conventional LBE and DFS but different numerical approaches are used to achieve incompressibility. For Case C where the flow is subject to temperature and salinity stratification,

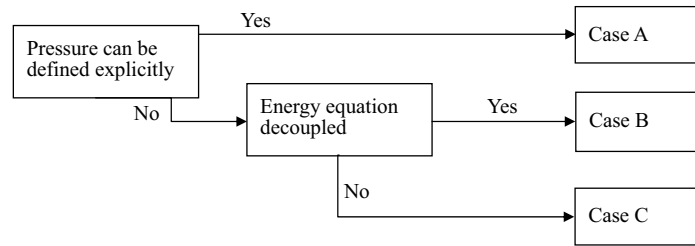


Figure 2: Illustration chart for the three cases.

conventional LBE, which inherently assumes an ideal gas law, is not applicable because the fluid is a liquid; however, the present DFS is still valid because there is no restriction on the property of the fluid considered. The relation between the general DFS, the conventional LBE and these three cases is illustrated in Fig. 2.

Once the mathematical framework for the DFS and its equivalency to the BGK-type modeled LBE has been established, the finite difference scheme of [5, 11, 13], which consists of a streaming and a diffusive step [29] is again used to numerically solve the \tilde{f}_α and \tilde{g}_α lattice equations. For incompressible flows, the iterative scheme of [25] is adopted so that the constant ρ assumption can be satisfied. This iterative scheme is based on the pressure-correction method proposed in [31]. For ease of reference, the present finite difference numerical scheme is designated FDLBM/2 to indicate that the method solves two distribution functions, \tilde{f}_α and \tilde{g}_α , and to differentiate it from the FDLBM used in [5, 11, 13], which solves the lattice equations governing the transport of the distribution function \tilde{f}_α only.

3.1 Case A — Compressible flow with ideal gas law

In this case, p can be explicitly expressed as a function of ρ and e (or T) through an equation of state, or by invoking a compressibility relation. The case with an ideal gas law is chosen as an illustrative example. As explained in the Introduction, the mass, momentum and energy equations are coupled in a compressible flow. If an equation of state is specified, solving Eqs. (2.5) and (2.12) simultaneously is equivalent to solving the full set of NS equation. However, the current case does not include a complicated thermodynamics equation of state; such as the case where p , ρ and T are related by a differential equation with temporal derivative, or p is defined implicitly by other state variables. This point is further discussed in Case C.

It should be noted that e_t is the sum of e and the flow kinetic energy $\rho|\mathbf{u}|^2/2$. Under the present formulation, the kinetic energy can be expressed in terms of f_α . This suggests that g_α can be related to f_α if a relation between p , ρ and e is available. In other words, a way to simplify the two-distribution-function DFS approach to a single-distribution-function formulation of the conventional LBE could be found, and this means that only one distribution function is sufficient to represent particle dynamics as suggested in ki-

netic theory of gases. In order to establish this connection, according to [11, 13], Eq. (2.7c) is modified to read

$$\sum_{\alpha} f_{\alpha}^{eq}(\xi_{\alpha})_i(\xi_{\alpha})_j = \rho u_i u_j + p \delta_{ij} - \tau_{ij} + P'_{ij}, \quad (3.1)$$

such that

$$\frac{\partial P'_{ij}}{\partial x_j} = 0, \quad (3.2)$$

and P'_{ij} is a dimensionless second-order tensor. This condition is necessary if the correct momentum equation were to be recovered [11, 13]. With the introduction of P'_{ij} in Eq. (3.1), the problem of finding a relation between g_{α} and f_{α} is reduced to determining the behavior of P'_{ij} that permits such a relation to exist. From Eq. (3.1), it can be shown that

$$\sum_{\alpha} \frac{1}{2} f_{\alpha}^{eq} |\xi_{\alpha}|^2 = \frac{1}{2} \rho |\mathbf{u}|^2 + \frac{D}{2} p - \frac{1}{2} \sum_i \tau_{ii} + \frac{1}{2} \sum_i P'_{ii}, \quad (3.3)$$

where D is the dimension of the flow problem. For an ideal gas, p can be expressed in terms of ρ and e as $p = \rho e (\gamma - 1)$. Using Eqs. (2.10), (2.13a), and (2.13b), it can be shown that

$$\begin{aligned} \sum_{\alpha} g_{\alpha}^{eq} &= \sum_{\alpha} g_{\alpha} = \rho e + \frac{1}{2} \rho |\mathbf{u}|^2 \\ &= \frac{1}{2} \sum_{\alpha} f_{\alpha}^{eq} |\xi_{\alpha}|^2 - \rho e \left[\frac{D(\gamma-1)}{2} - 1 \right] + \frac{1}{2} \sum_i \tau_{ii} - \frac{1}{2} \sum_i P'_{ii}. \end{aligned} \quad (3.4)$$

Thus, g_{α} and g_{α}^{eq} can be written as

$$g_{\alpha} = \frac{1}{2} f_{\alpha} |\xi_{\alpha}|^2 \quad \text{and} \quad g_{\alpha}^{eq} = \frac{1}{2} f_{\alpha}^{eq} |\xi_{\alpha}|^2, \quad (3.5)$$

if $\sum_i P'_{ii}$ satisfies the following condition,

$$\sum_i P'_{ii} = -\rho e [D(\gamma-1) - 2] + \sum_i \tau_{ii}. \quad (3.6)$$

An expression for p can now be deduced from Eqs. (3.4), (3.5), and (3.6); the result is

$$p = (\gamma - 1) \left[\sum_{\alpha} \frac{1}{2} f_{\alpha} |\xi_{\alpha}|^2 - \frac{1}{2} \rho |\mathbf{u}|^2 \right]. \quad (3.7)$$

Consequently, for an ideal gas, there is no need to consider a second particle distribution function; only one is needed to establish the equivalency of the LBE with the NS equations.

Besides the relations given in Eqs. (3.5), if the result given in [11,13] is to be recovered, Eq. (3.4) has to be re-written as:

$$\begin{aligned} \frac{D(\gamma-1)}{2} \sum_{\alpha} g_{\alpha}^{eq} &= \frac{D(\gamma-1)}{2} \sum_{\alpha} g_{\alpha} = \frac{D(\gamma-1)}{2} \left[\rho e + \frac{1}{2} \rho |\mathbf{u}|^2 \right] \\ &= \frac{1}{2} \sum_{\alpha} f_{\alpha}^{eq} |\xi_{\alpha}|^2 + \frac{1}{2} \rho |\mathbf{u}|^2 \left[\frac{D(\gamma-1)}{2} - 1 \right] + \frac{1}{2} \sum_i \tau_{ii} - \frac{1}{2} \sum_i P'_{ii}. \end{aligned} \quad (3.8)$$

The relations between g_{α} and g_{α}^{eq} , and f_{α} are then given by

$$g_{\alpha} = \frac{1}{D(\gamma-1)} f_{\alpha} |\xi_{\alpha}|^2 \quad \text{and} \quad g_{\alpha}^{eq} = \frac{1}{D(\gamma-1)} f_{\alpha}^{eq} |\xi_{\alpha}|^2, \quad (3.9)$$

provided P'_{ii} satisfies the condition

$$\sum_i P'_{ii} = \rho |\mathbf{u}|^2 \left[\frac{D(\gamma-1)}{2} - 1 \right] + \sum_i \tau_{ii}. \quad (3.10)$$

Therefore, using Eqs. (3.9) and (3.10), Eq. (3.8) can be solved to yield an expression for p , i.e.,

$$p = \sum_{\alpha} \frac{1}{D} f_{\alpha} |\xi_{\alpha}|^2 - \frac{(\gamma-1)}{2} \rho |\mathbf{u}|^2. \quad (3.11)$$

However, in both cases, a more general expression for p can be deduced as

$$p = \sum_{\alpha} \frac{1}{D} f_{\alpha} |\xi_{\alpha}|^2 - \frac{1}{2} \rho |\mathbf{u}|^2 + \frac{1}{D} \sum_i \tau_{ii} - \frac{1}{D} \sum_i P'_{ii}. \quad (3.12)$$

This analysis provides a meaning for P'_{ij} which has not been explained fully in [11,13]. It has to be introduced into Eq. (2.7c) so that a condition can be established for the recovery of the NS equations from one single particle distribution function. The two different approaches give rise to two slightly different relations between g_{α} and f_{α} . The exact choice is not important because the difference is only in the coefficient qualifying the relation between g_{α} and f_{α} .

Linking g_{α} to f_{α} and incorporating the constraints of g_{α}^{eq} into f_{α}^{eq} , it can be easily seen that solving Eq. (2.5) is sufficient to demonstrate equivalency with the NS equations; Eq. (2.12) is no longer required. As a result, only the transport of one distribution function f_{α} needs to be solved. The price is the solution of an additional Eq. (3.2) for P'_{ij} . The meaning of ε in Eq. (2.5) can then be interpreted as Kn and the expansion of f_{α} in Eq. (2.6) is in terms of Kn , much like the Chapman-Enskog expansion in LBM. It is reminded that g_{α} can be expressed in terms of f_{α} only if p can be expressed explicitly as a function of ρ and e . The present approach, without linking g_{α} with f_{α} , is more convenient because it does not require the exact specification of an equation of state for the fluid. It does,

however, require the solution of two BGK-type equations for the distribution functions f_α and g_α .

Finally, it should be pointed out that the choice of Eqs. (3.9) and (3.10) is exactly equivalent to a previous FDLBM formulation for compressible viscous flow given in [11, 13]. The previous FDLBM has been applied to shock capturing problems as well as to simulate shock structures, and to resolve acoustic scattering by a vortex and by an isolated heat source [10–13]. Good agreement with direct numerical simulation results and analytical solutions is obtained. In the previous treatment [11, 13], P'_{ij} is introduced in Eqs. (3.1) and (3.2) to provide flexibility for an equation of state for diatomic gas; otherwise, only the flow of three-dimensional (3-D) Newtonian monatomic gas is applicable (because in such a case, $\sum \tau_{ii} = 0$, $D = 3$, $\gamma = 5/3$, and $P'_{ij} = 0$ will always be a solution).

Case B – Incompressible isothermal and non-isothermal flow

Incompressible flow can be specified by $D\rho/Dt = 0$. As a result, the mass conservation equation, Eq. (2.9a), is reduced to $\nabla \cdot \mathbf{u} = 0$, which is equivalent to saying that volume is preserved. Therefore, constant density is a sufficient condition for the flow to be incompressible and this is the case considered here. For the isothermal case, there is no need to solve the energy equation because the temperature T is also a constant. Only the mass and momentum equations need be solved. For the non-isothermal case, as long as the energy equation is decoupled from the mass and momentum equations, once the velocity and pressure fields are known, the energy (or the g_α) equation can be solved separately. In the following discussion, emphasis is placed on the solution of f_α for an incompressible flow where $D\rho/Dt = 0$ is valid in the whole flow field.

When ρ is a constant, it becomes a parameter rather than a solution of the NS equations. The pressure p is, instead, treated as a dependent variable and is a part of the solution of the NS equations; it cannot be explicitly expressed as a function of other parameters and variables. Consequently, an expression for p has to be found from f_α . By hint of Eq. (3.12), an expression for p is given by

$$p = \sum_{\alpha} \frac{1}{D} f_{\alpha} |\xi_{\alpha}|^2 - \frac{1}{D} \rho |\mathbf{u}|^2 + \frac{1}{D} \sum_i \tau_{ii}, \quad (3.13)$$

and the average or mechanical pressure is then defined as

$$\bar{p} = p - \frac{1}{D} \sum_i \tau_{ii} = \sum_{\alpha} \frac{1}{D} f_{\alpha} |\xi_{\alpha}|^2 - \frac{1}{D} \rho |\mathbf{u}|^2. \quad (3.14)$$

The right hand side (RHS) of Eq. (3.14) shows that, in this definition, the mechanical pressure is the difference between the second moment of f_α and the kinetic energy. For incompressible flow, solving Eq. (2.5) with the help of Eqs. (2.3b) and (3.13) may not necessarily satisfy Eq. (2.3a). Therefore, it is necessary to develop an iterative numerical method to ensure the fulfillment of Eq. (2.3a) while these other equations are being solved simultaneously.

In order to accomplish this objective, a slightly modified form of Eq. (2.5) is solved, i.e.,

$$\frac{\partial f'_\alpha}{\partial t'} + \frac{\partial f_\alpha}{\partial t} + \boldsymbol{\xi}_\alpha \cdot \nabla f_\alpha = -\frac{f_\alpha - f_\alpha^{eq}}{\varepsilon\tau}. \quad (3.15)$$

The time t is now treated as a pseudo time for iteration until Eqs. (2.3a), (2.3b) and (3.13) are all satisfied, while t' is the physical time, and f'_α is defined such that

$$\sum_\alpha f'_\alpha = \rho, \quad (3.16a)$$

$$\sum_\alpha f'_\alpha \boldsymbol{\xi}_\alpha = \rho \mathbf{u}, \quad (3.16b)$$

$$\sum_\alpha \frac{1}{D} f'_\alpha |\boldsymbol{\xi}_\alpha|^2 = \frac{c^2 \rho}{D}. \quad (3.16c)$$

In addition to Eqs. (2.7a)-(2.7c), f_α^{eq} also has to satisfy the constraint,

$$\sum_\alpha \frac{1}{D} f_\alpha^{eq} |\boldsymbol{\xi}_\alpha|^2 \boldsymbol{\xi}_\alpha = \frac{c^2 \rho \mathbf{u}}{D}. \quad (3.17)$$

Multiplying Eq. (3.15) with respect to $\{1, \boldsymbol{\xi}_\alpha, |\boldsymbol{\xi}_\alpha|^2/D\}^T$, taking summation over α , and using Eqs. (2.3b) and (3.13), the following equations are obtained,

$$\frac{\partial \rho}{\partial t'} + \frac{\partial}{\partial t} \left(\sum_\alpha f_\alpha \right) + \sum_j \frac{\partial \rho u_j}{\partial x_j} = -\frac{1}{\varepsilon} \left(\sum_\alpha f_\alpha - \rho \right), \quad (3.18a)$$

$$\frac{\partial(\rho u_i)}{\partial t'} + \frac{\partial(\rho u_i)}{\partial t} + \sum_j \frac{\partial}{\partial x_j} (\rho u_i u_j + p \delta_{ij} + \tau_{ij}) = \mathcal{O}(\varepsilon), \quad (3.18b)$$

$$\frac{\partial}{\partial t} \left[p - \frac{1}{D} \sum_j \tau_{jj} + \frac{1}{D} \rho |\mathbf{u}|^2 \right] + \frac{c^2}{D} \left(\frac{\partial \rho}{\partial t'} + \sum_j \frac{\partial \rho u_j}{\partial x_j} \right) = \mathcal{O}(\varepsilon). \quad (3.18c)$$

After steady state has been reached with respect to the pseudo time, Eqs. (3.18b) and (3.18c) become the momentum and the mass conservation equation of the NS equations. Furthermore, due to Eq. (3.18a), Eq. (2.3a) is also satisfied. The first bracketed term in Eq. (3.18c) is the pseudo time rate of change of the "mechanical pressure" plus the "dynamic pressure", which can be denoted as the "total pressure head". The second bracketed term in Eq. (3.18c) is essentially the LHS of Eq. (2.9a). Since ρ is constant, this term becomes the divergence of the velocity multiplying by a factor $(\rho c^2/D)$, which is the "dynamic pressure" or the "kinetic energy" due to the chosen speed c . The divergence of the velocity can be viewed as "the time rate of change of the volume of a moving fluid element per volume"; therefore, Eq. (3.18c) could be viewed as a pressure-correction formula to correct the "total pressure head" by balancing it with the time rate of change of the volume, until the change is negligibly small, which in fact, is the definition of an incompressible flow. The above technique is similar to the pressure-correction method of [31].

For non-isothermal flows, the energy equation is decoupled from the mass and momentum equations; therefore, it can be solved separately. The velocity and pressure fields are obtained by solving the f_α equation, while g_α can be deduced by solving Eqs. (2.10)-(2.15) and hence e (or T). This pressure-correction technique for incompressible flow has been previously presented [25] and used to simulate incompressible flows in 2-D channels and micro-channels, in flow over a cavity, and in sudden expansion flow [5]. Good agreement with analytical and known numerical results is obtained.

Case C — Stratified flow

A geophysical fluid dynamics problem, such as a double diffusive flow in the ocean, is chosen as an example to illustrate the extension of the DFS to incompressible flow with energy equation coupling. For a stratified flow with Boussinesq approximation, the mean density is considered constant as far as its mass is concerned; however, density variation is retained in the buoyancy term of the governing equations. Consequently, ρ can be written as $\rho = \rho_0 + \rho'$, where ρ_0 is a constant reference density, and $\rho' \ll \rho_0$ is the density disturbance. The governing equations are given by

$$\frac{\partial u_j}{\partial x_j} = 0, \quad (3.19a)$$

$$\rho_0 \left(\frac{\partial u_i}{\partial t} + \frac{\partial u_i u_j}{\partial x_j} \right) = - \frac{\partial p}{\partial x_i} + \mu \frac{\partial^2 u_i}{\partial x_j \partial x_j} - \rho' g \delta_{i3} - \rho_0 (2\omega_i \times u_i), \quad (3.19b)$$

where g is the gravitational acceleration, and $2\omega_i \times u_i$ is the Coriolis acceleration due to earth's rotation, whose angular velocity is given by ω_i . The density of seawater in the ocean is affected not only by temperature, but also by salinity S . As a first approximation, a linear equation between ρ , T and S can be adopted [32]

$$\rho = \rho_0 [1 - \beta_1 (T - T_0) + \beta_2 (S - S_0)], \quad (3.20)$$

where β_1 is the coefficient of thermal expansion, β_2 is the coefficient of saline contraction, and ρ_0 , T_0 , S_0 are reference values. The temperature and the salinity are governed by the following transport equations, respectively,

$$\frac{\partial T}{\partial t} + \mathbf{u} \cdot \nabla T = k_T \nabla^2 T, \quad (3.21a)$$

$$\frac{\partial S}{\partial t} + \mathbf{u} \cdot \nabla S = k_S \nabla^2 T. \quad (3.21b)$$

With the help of $\nabla \cdot \mathbf{u} = 0$, they can be written in conservation form; therefore, they can be solved using the method developed for g_α as detailed in Eqs. (2.10)-(2.15). Density disturbance can be assessed using Eqs. (3.20), (3.21a), and (3.21b) or simply by solving

$$\frac{\partial \rho'}{\partial t} + \mathbf{u} \cdot \nabla \rho' = k_T \nabla^2 \rho', \quad (3.22)$$

which can again be treated using the method developed for g_α .

This case is different from Case B because the salinity equation and the momentum equation is coupled through ρ' ; therefore, the method of Case B for incompressible flow alone is not adequate. In order to solve this problem, Eq. (3.15) needs to be modified by the inclusion of a body force term to give,

$$\frac{\partial f'_\alpha}{\partial t'} + \frac{\partial f_\alpha}{\partial t} + \boldsymbol{\zeta}_\alpha \cdot \nabla f_\alpha + F_\alpha = -\frac{f_\alpha - f_\alpha^{eq}}{\varepsilon\tau}, \quad (3.23)$$

where F_α is added to account for the presence of the gravitational and Coriolis force term in Eq. (3.19b). It can be seen that F_α contains ρ' and this can be determined by solving Eqs. (3.20), (3.21a), and (3.21b) or by solving Eq. (3.22) directly. The distribution functions f'_α and f_α^{eq} are as defined in Case B, except that ρ is now replaced by ρ_0 . For every pseudo time step Δt , solving Eq. (3.23) gives an update to the velocity field. Using this updated velocity, a corrected ρ' can be determined from Eqs. (3.20) and (3.21) or from Eq. (3.22), which then provides an updated F_α . The iteration process continues until a steady state with respect to the pseudo time has been reached. Consequently, the divergence of the velocity field ($\nabla \cdot \mathbf{u} = 0$) is satisfied and so is Eq. (3.18c).

In principle, the same algorithm can be applied to flows without invoking the Boussinesq approximation or with a more complicated state equation. For example, instead of Eq. (3.20), a state equation [32] that is commonly adopted for oceanographic flow is

$$\rho(T, S, p) = \rho(T, S, 0) = \left[1 - \frac{p}{K(T, S, p)} \right]^{-1}, \quad (3.24)$$

where $\rho(T, S, 0)$ and $K(T, S, p)$ are complicated functions of T , S and p , and are given by

$$\begin{aligned} \rho(T, S, 0) = & 999.842594 + 6.793952 \times 10^{-2} T - 9.095290 \times 10^{-3} T^2 + \dots \\ & - 1.6546 \times 10^{-6} T^2 S^{1.5} + 4.83140 \times 10^{-4} S^2, \end{aligned} \quad (3.25a)$$

$$\begin{aligned} K(T, S, p) = & 19652.21 + 148.4206 T - 2.327105 T^2 + \dots \\ & - 2.0816 \times 10^{-3} T p^2 S + 9.1697 \times 10^{-10} T^2 p^2 S. \end{aligned} \quad (3.25b)$$

Although a state equation relating ρ , T , p , and S is now available, the pressure still cannot be defined explicitly. Therefore, the method of Case A is not applicable. Since the salinity equation is coupled to the momentum equation, the method of Case B is also not applicable. Thus, the problem is different from the previously treated stratified flow because the density can no longer be approximated by a constant, and the conservation of mass needs to be satisfied rather than the conservation of volume. The same algorithm can again be used because the conservation of mass can be assured by Eq. (3.18c) after a steady state has been reached in the pseudo time. In every pseudo time step, ρ in f_α^{eq} and f'_α is updated by Eq. (3.24)-(3.25b). An iteration process similar to that previously employed is adopted; thus ensuring mass conservation and the satisfaction of Eq. (3.18c).

4 Velocity lattice model and numerical scheme for FDLBM/2

A velocity lattice method is used to solve the f_α and g_α equations, i.e., Eqs. (2.5) and (2.12), respectively, in the present FDLBM/2 for incompressible, non-isothermal flows. The method used is the same for the f_α and g_α equations; it is only necessary to give a brief outline on the solution of these equations. In the present investigation, a Cartesian coordinate system with x - and y -axis to represent the stream and normal direction is assumed for two-dimensional (2-D) flows. Following the work of [5, 10–13], a two-dimensional, nine lattice (D2Q9) velocity lattice model is assumed for f_α and g_α . Extension to 3-D flows is straightforward and is given in detail in [28]. In line with [5, 10–13], a second order polynomial in ξ_α is assumed for f_α^{eq} and a first order one for g_α , i.e.,

$$f_\alpha^{eq} = A_\alpha + (\xi_\alpha)_x Ax_\alpha + (\xi_\alpha)_y Ay_\alpha + (\xi_\alpha)_x^2 Bxx_\alpha + (\xi_\alpha)_y^2 Byy_\alpha + (\xi_\alpha)_x (\xi_\alpha)_y Bxy_\alpha, \quad (4.1a)$$

$$g_\alpha^{eq} = C_\alpha + (\xi_\alpha)_x Cx_\alpha + (\xi_\alpha)_y Cy_\alpha, \quad (4.1b)$$

where the coefficients, A_α , Ax_α , Ay_α , Bxx_α , C_α , etc, need to be determined. These coefficients are determined by invoking Eqs. (2.7a)-(2.7c), and (2.13a), (2.13b), and the conditions that higher moments of f_α^{neq} and g_α^{neq} vanish. Their values for a D2Q9 model are determined by assuming the lattice distribution and its magnitude to be given by

$$\xi_0 = 0, \quad \alpha = 0, \quad (4.2a)$$

$$\xi_\alpha = \sigma \left\{ \cos \left[\frac{\pi(\alpha-1)}{4} \right], \sin \left[\frac{\pi(\alpha-1)}{4} \right] \right\}, \quad (4.2b)$$

$$\xi_\alpha = \sqrt{2}\sigma \left\{ \cos \left[\frac{\pi(\alpha-1)}{4} \right], \sin \left[\frac{\pi(\alpha-1)}{4} \right] \right\}, \quad (4.2c)$$

where σ is a parameter whose value is dependent on the problem and the numerical method [28].

If the coefficients having the same "energy shell" of the lattice velocities are assumed identical, the number of unknowns resulting from the coefficients, A_α , Ax_α , Bxx_α , C_α , etc, exceed the available constraints for f_α and g_α in a D2Q9 lattice model. Six constraints are available for the determination of the coefficients for f_α , and three are available for g_α . Consequently, assumptions are necessary in order to facilitate the determination of these coefficients. As a first attempt, seven and four coefficients for f_α and g_α , respectively, are assumed zero. The results are:

$$A_0 = \rho - \frac{2p}{\sigma^2} - \frac{\rho|\mathbf{u}|^2}{\sigma^2} + \frac{\tau_{xx} + \tau_{yy}}{\sigma^2}, \quad A_1 = A_2 = 0, \quad (4.3a)$$

$$Ax_1 = \frac{\rho u}{2\sigma^2}, \quad Ax_2 = 0, \quad (4.3b)$$

$$Ay_1 = \frac{\rho v}{2\sigma^2}, \quad Ay_2 = 0, \quad (4.3c)$$

$$Bxx_1 = \frac{1}{2\sigma^4}(p + \rho u^2 - \tau_{xx}), \quad Bxx_2 = 0, \quad (4.3d)$$

$$Byy_1 = \frac{1}{2\sigma^4}(p + \rho v^2 - \tau_{yy}), \quad Byy_2 = 0, \quad (4.3e)$$

$$Bxy_2 = \frac{1}{4\sigma^4}(\rho uv - \tau_{xy}), \quad Bxy_1 = 0, \quad (4.3f)$$

$$C_0 = \rho e_t, \quad C_1 = C_2 = 0, \quad (4.3g)$$

$$Cx_1 = \frac{1}{2\sigma^2}[u(p + \rho e_t) + u\tau_{xx} + v\tau_{xy} + q_x], \quad Cx_2 = 0, \quad (4.3h)$$

$$Cy_1 = \frac{1}{2\sigma^2}[v(p + \rho e_t) + u\tau_{xy} + v\tau_{yy} + q_y], \quad Cy_2 = 0, \quad (4.3i)$$

where u and v are the velocity components along the x - and y -direction, respectively. The value of σ is estimated depending on the numerical method used to solve the lattice equations. The details for different flow types are given in [5, 10–13, 28]. Thus determined, the coefficients are not unique; other assumptions could be made for the zero coefficients. The results given in Eqs. (4.3a)-(4.3i) might change as a result. However, the studies of [5, 10–13, 28] have shown that this assumption seems to work best for the different incompressible, isothermal and non-isothermal, and compressible flow investigations carried out so far.

Different numerical schemes can be used to solve Eqs. (2.5) and (2.12) with a velocity lattice model given by Eqs. (4.1a)-(4.3i). The order of accuracy of the numerical schemes used depends to a great extent on the physical problem and on whether the flow is compressible or incompressible. Even for compressible flows, the order of the numerical scheme also differs. For example, a sixth-order scheme is necessary if the acoustics disturbances were to be resolved correctly, such as in the acoustics propagation and acoustics-scattering problems treated in [9–11]. On the other hand, for shock capturing [12] problems, a shock capturing scheme such as the total variation diminishing scheme is required. Otherwise, the numerical simulation will be too cumbersome and could even lead to numerical instability. For shock structure problems, usually a second-order accurate numerical scheme is sufficient; however, in order to obtain better accuracy, a 6th-order Lele scheme [13] is used in the present FDLBM/2 simulation. In the case of incompressible flow, irrespective whether the energy equation is coupled with the mass and momentum equation, a pressure-correction method [25] is required in order to ensure constant-density behavior in the flow [5]. In spite of these differences, there is one commonality among these numerical schemes; i.e., they all used a splitting method, finite difference scheme to solve Eqs. (2.5) and (2.12). The splitting method [29] is a common tool for time dependent convective-diffusive type differential equations. The governing equation is split into a convective part and a diffusive part; thus, its solution is divided into two steps. The first step solves the convective part with specified initial conditions for the dependent variable, while the second step solves the diffusive part using the solution of the convective part as initial conditions for the diffusive equation. Details of the splitting method, numerical scheme for compressible flows are given in [11–13]; for

incompressible flows they are provided in [5, 25].

For the sake of completeness, a brief description of the splitting technique for incompressible, non-isothermal flows is given below to serve as reference for interested readers:

- i. Initial macroscopic quantities are used to calculate the initial f_α^{eq} and g_α^{eq} , which are then used as initial values to start the calculation.
- ii. With f_α and g_α at time t known, intermediate values f_α^I and g_α^I are calculated from the convective equations,

$$\frac{\partial f_\alpha}{\partial t} + \xi_\alpha \cdot \nabla f_\alpha = 0, \quad (4.4a)$$

$$\frac{\partial g_\alpha}{\partial t} + \xi_\alpha \cdot \nabla g_\alpha = 0, \quad (4.4b)$$

which can be solved by any time marching finite difference scheme.

- iii. Using this f_α^I and g_α^I , the corresponding intermediate macroscopic quantities (u_I, v_I, p_I, e_{tI}) for all interior grid points are calculated as

$$u_I \equiv \frac{1}{\rho} \sum_{\alpha=0}^8 f_\alpha^I (\xi_\alpha)_x, \quad v_I \equiv \frac{1}{\rho} \sum_{\alpha=0}^8 f_\alpha^I (\xi_\alpha)_y, \quad (4.5a)$$

$$p_I \equiv \sum_{\alpha=0}^8 f_\alpha^I \frac{1}{2} \left((\xi_\alpha)_x^2 + (\xi_\alpha)_y^2 \right) - \frac{1}{2} \rho |\mathbf{u}_I|^2 + \frac{(\tau_{xx})_I + (\tau_{yy})_I}{2}, \quad (4.5b)$$

$$\rho_I = \sum_{\alpha} f_\alpha^I, \quad (4.5c)$$

$$e_{tI} = \frac{1}{\rho} \sum_{\alpha} g_\alpha^I. \quad (4.5d)$$

Either Eq. (4.5b) or (4.5c) is employed, which is case dependent, to find the pressure or the density, while the other quantity is found by the equation of state. For example, for incompressible flow (Case B), Eq. (4.5b) is employed to find the pressure. Then the density is assigned as a constant parameter (constant density can be treated as the equation state of an incompressible flow), and Eq. (4.5c) would be satisfied by iteration.

- iv. The boundary conditions for the macroscopic level are then set as in any finite difference methods.
- v. Using the macroscopic quantities thus determined, corresponding $f_\alpha^{I,eq}$ and $g_\alpha^{I,eq}$ values are obtained.
- vi. Using f_α^I and g_α^I as the initial condition, the diffusion equations

$$\frac{\partial f_\alpha}{\partial t} = -\frac{1}{\tau Kn} (f_\alpha - f_\alpha^{eq}), \quad (4.6a)$$

$$\frac{\partial g_\alpha}{\partial t} = -\frac{1}{\tau Kn} (g_\alpha - g_\alpha^{eq}), \quad (4.6b)$$

are solved. The scheme makes use of the advantage of an arbitrary relaxation time. By setting $\tau=1$ and $Kn=\Delta t$, it can be shown that f_α and g_α at time $(t+\Delta t)$ are exactly the same as $f_\alpha^{I,eq}$ and $g_\alpha^{I,eq}$ (see [25] for details); hence, $(u,v,p,e_t)|_{t+\Delta t}=(u_I,v_I,p_I,e_{tI})$.

vii. Time marching proceeds by repeating procedures (ii) to (vi).

Similarly, for compressible and other types of flows, the procedure follows closely that given above (for further details, refer to [11–13,28]).

5 Numerical simulation examples

The FDLBM of [11, 13] has been used to simulate aeroacoustic propagation and acoustic scattering problems and good agreement with other known data was obtained [10, 11]. Further, the approach has been used to simulate shock structure of monatomic and diatomic gases at $M \cong 1.5$ (see [13]). In [13], shock structure problems were chosen because the objective was to demonstrate that, apart from the NS equations, the FDLBM can be extended to treat a more complicated flow model, e.g., models with nonlinear transport coefficients, and with an extended thermodynamics model, such as the Brenner-Navier-Stokes model [33–35]. On the other hand, the FDLBM/2 has been used to simulate a series of incompressible, non-isothermal gas and liquid flows in two and three dimensions, and good agreement with analytical results and other known numerical simulations was obtained [28]. Since the present DFS formulation of the FDLBM/2 has been demonstrated to be equivalent to the FDLBM with an equation of state stipulated, there is no doubt that the FDLBM/2 simulations of the aeroacoustic and non-isothermal problems will be identical to those derived from the FDLBM [10–13]. Consequently, it is not necessary to repeat the same simulations again using FDLBM/2. In order to verify the soundness of the FDLBM/2 for shock structure simulations and thus demonstrating that the method can also be extended to simulate a more complicated flow model, such as the Brenner-Navier-Stokes model [33–35], the FDLBM/2 is used to simulate the measured Argon and Nitrogen shock structures reported in [36] and the results compared with the measurements and those deduced from the FDLBM reported in [13].

In order to demonstrate the viability and validity of the FDLBM/2 for oceanographic flow, the FDLBM/2 is used to simulate a double diffusive phenomenon in a rectangle reported in [37, 38]. This calculation is chosen to further demonstrate the validity and extent of the FDLBM/2 for liquid flow simulation. If possible, the calculations are compared with other known numerical results [37, 38]. Therefore, in the current work, only two numerical simulations are reported; one on shock structure and another on double diffusive phenomenon in a rectangle.

5.1 Shock structure simulation using FDLBM/2

Since the continuum NS equations are not appropriate for flows with a finite Kn (of the order of $\cong 0.2$) such as found in shock structure at relatively high M , a correction to the

NS equations has been proposed by Brenner [33, 34]. This correction has been tested in [35]. The calculated shock structure profiles obtained by numerically solving the Brenner corrected NS equations were in good agreement with experimental data [36] for Argon gas but not for Nitrogen gas. The FDLBM using a single distribution function has been revised to recover the Brenner corrected NS equations [13] and the simulated results were compared with the measurements of [36] and the finite difference solution of the NS equations with the Brenner correction [13]. The results thus obtained showed that the FDLBM simulations are essentially identical to those deduced directly from the NS equations with the Brenner correction. In order to further demonstrate the equivalency between the FDLBM and the FDLBM/2 approaches, the same shock structure problems are again solved using the FDLBM/2 and the results are compared with those reported in [13]. For the sake of completeness, the Brenner corrected NS equations are given below without showing how they were obtained; details are given in [35]. The Brenner corrected NS equations are:

$$\frac{\partial \rho}{\partial t} + \frac{\partial}{\partial x_j}(\rho u_j) = 0, \quad (5.1a)$$

$$\frac{\partial(\rho u_i)}{\partial t} + \frac{\partial}{\partial x_j}(p \delta_{ij} + \rho u_i u_j - T_{ij}) = 0, \quad (5.1b)$$

$$\frac{\partial}{\partial t} \left(\rho e + \frac{1}{2} \rho |\mathbf{u}|^2 \right) + \frac{\partial}{\partial x_j} \left[u_j \left(p + \rho e + \frac{1}{2} \rho |\mathbf{u}|^2 \right) - u_k T_{jk} - \frac{\gamma M}{Pr Re} \frac{\partial e}{\partial x_j} - \frac{M}{Pr_b Re} \frac{\mu p}{\rho^2} \frac{\partial \rho}{\partial x_j} \right] = 0, \quad (5.1c)$$

where the stress tensor has been modified by adding an additional term and the resulting expression is given by

$$T_{ij} = \frac{\mu M}{Re} \left(\frac{\partial u_j}{\partial x_i} + \frac{\partial u_i}{\partial x_j} \right) + \frac{\lambda M}{Re} \left(\frac{\partial u_k}{\partial x_k} \right) \delta_{ij} + B_{ij}, \quad (5.2a)$$

$$B_{ij} = \left\langle \frac{2\mu M^2}{Re^2 Pr_b} \frac{\partial}{\partial x_i} \left(\frac{\mu}{\rho^2} \frac{\partial \rho}{\partial x_j} \right) \right\rangle. \quad (5.2b)$$

The angle bracket is defined as

$$\langle A \rangle = A'' - \frac{1}{3} \text{tr}(A'') I, \quad A'' = \frac{1}{2} (A + A^T), \quad (5.3)$$

and λ and Pr_b are the second viscosity coefficient and a second Prandtl number introduced by Brenner. Finally, the viscosity coefficient μ is modeled by a power law with an exponent s .

The FDLBM/2 results and their comparisons with measurements [36] and the FDLBM simulations [13] are shown in Figs. 3 and 4. The numerical discretization used to solve the FDLBM equations [13] is also used here to solve the FDLBM/2 equations. For convenience, details of the numerical scheme are highlighted in the figure captions. The Argon shock structure profiles are plotted in Fig. 3; all numerical simulations, finite difference solution of the Brenner corrected NS equations, the FDLBM and FDLBM/2 calculations, are essentially identical, and are in very good agreement with the measurements of [36]. The Nitrogen shock structure results are shown in Fig. 4. As expected, the three numerical simulations are essentially identical; however, they are not in agreement with the

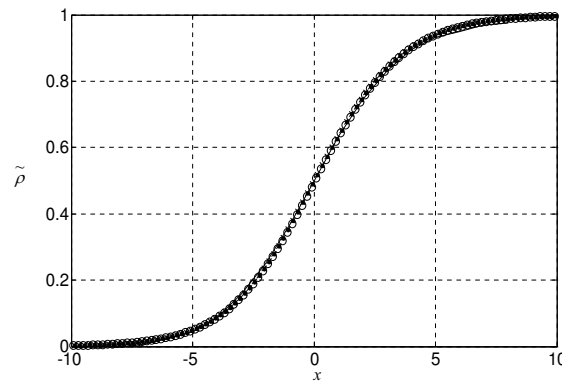


Figure 3: Shock structure profile for Argon gas at $M=1.55$ with $Pr=2/3$, $Pr_b=1$, $\gamma=5/3$, $\lambda=-2/3\mu$, and $s=0.816$: "—" measurements [36]; "x" numerical result from solving Brenner corrected NS equations using finite difference method (4th order Runge-Kutta for temporal and 6th order Lele compact scheme for spatial with $\Delta x=0.2$, and $\Delta t=0.001$); "•" FDLBM (2nd order Runge-Kutta for temporal and 6th order Lele compact scheme for spatial with $\Delta x=0.2$, and $\Delta t=0.01$); "o" FDLBM/2 (same numerical discretization scheme as the FDLBM case).

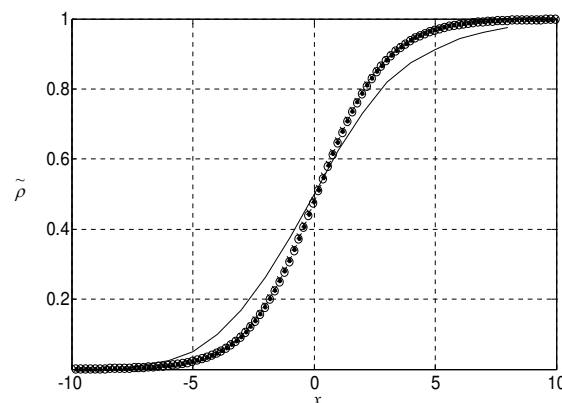


Figure 4: Shock structure profile for Nitrogen gas at $M=1.53$ with $Pr=0.71$, $Pr_b=1$, $\gamma=1.4$, $\lambda=-2/3\mu$, and $s=0.756$: "—" measurements [36]; "x" numerical result from solving Brenner corrected NS equations using finite difference method (4th order Runge-Kutta for temporal and 6th order Lele compact scheme for spatial with $\Delta x=0.2$, and $\Delta t=0.001$); "•" FDLBM (2nd order Runge-Kutta for temporal and 6th order Lele compact scheme for spatial with $\Delta x=0.2$ and $\Delta t=0.01$); "o" FDLBM/2 (same numerical discretization scheme as the FDLBM case).

measurements of [36]. These comparisons show that the FDLBM/2 and FDLBM results are identical, and are as good as the results of the Brenner corrected NS equations. The results further show that the NS equations, with or without the Brenner correction, are not suitable for flows with finite Kn such as found in shock structures of diatomic gas at relatively high M (in this case $M=1.5$, and $Kn \approx 0.2$). Therefore, the FDLBM and the FDLBM/2, which recover the Brenner corrected NS equations, also cannot be used to simulate flows with finite Kn .

5.2 Double diffusive phenomenon in a rectangle

It should be pointed out that the present formulation is valid for laminar flows only. As such the numerical analysis of double diffusion in a rectangle [37, 38] is limited to situations where the Rayleigh number cannot be too large; otherwise, the flow will become turbulent and the numerical calculation will become unstable. The main difficulty of this kind of simulation is that excessively large computational resources are required to resolve the thin solutal boundary layer. A highly stretched non-uniform grid was used in [37]. As a preliminary attempt to demonstrate the validity and extent of FDLBM/2, a uniform grid is chosen for the present study. In order to obtain a stable simulation, the double diffusive phenomenon in a rectangle is carried out using the same geometric and physical specifications of [37], except a smaller Rayleigh number is chosen instead. Therefore, a quantitative comparison of the present calculations with the numerical results of [37] cannot be made; only a qualitative comparison can be attempted. This does not represent a drawback because, after all, one of the current objectives is to evaluate the validity and extent of the DFS formulation as an alternative to the NS equations for double diffusive phenomenon.

Double-diffusive phenomena usually refer to a class of fluid motions which are subject to the simultaneous presence of two diffusive components with different molecular diffusivities. Much of the research on this topic is devoted to the oceanic flow process. The governing equations are the two-dimensional NS equations with Boussinesq approximations. The normalization and non-dimensional parameters employed are

$$x, y = \frac{\tilde{x}, \tilde{y}}{l_0}, \quad u, v = \frac{\tilde{u}, \tilde{v}}{\sqrt{R_T \kappa} / l_0}, \quad t = \frac{\tilde{t}}{l_0 / (\sqrt{R_T \kappa} / l_0)}, \quad (5.4a)$$

$$p = \frac{\tilde{p}}{\rho_0 (\sqrt{R_T \kappa} / l_0)^2}, \quad T = \frac{\tilde{T} - T_0}{\Delta T}, \quad S = \frac{\tilde{S} - S_0}{\Delta S}, \quad (5.4b)$$

$$R_T = \frac{g \beta_T \Delta T l_0^3}{\nu \kappa}, \quad R_S = \frac{g \beta_S \Delta S l_0^3}{\nu \kappa}, \quad R_\rho = \frac{R_S}{R_T}, \quad Pr = \frac{\nu}{\kappa}, \quad Le = \frac{\kappa}{\kappa_S}, \quad (5.4c)$$

where T and S are the temperature and salinity of the liquid, respectively, and ΔS and ΔT are their respective maximum differences across the cavity width. Other physical properties are: g , acceleration due to gravity; ν , kinematic viscosity; κ , thermal diffusivity; κ_S , diffusivity of the concentration; β_T and β_S , the coefficients of volume expansion of thermal and concentration differences, respectively. In the above definitions, R_T , R_S , Pr and Le are the thermal Rayleigh number, the solutal Rayleigh number, the Prandtl number and the Lewis number, respectively. The normalized governing equations are given by

$$\frac{\partial u}{\partial x} + \frac{\partial v}{\partial y} = 0, \quad (5.5a)$$

$$\frac{\partial u}{\partial t} + u \frac{\partial u}{\partial x} + v \frac{\partial u}{\partial y} = -\frac{\partial p}{\partial x} + \frac{Pr}{\sqrt{R_T}} \nabla^2 u, \quad (5.5b)$$

$$\frac{\partial v}{\partial t} + u \frac{\partial v}{\partial x} + v \frac{\partial v}{\partial y} = -\frac{\partial p}{\partial y} + \frac{Pr}{\sqrt{R_T}} \nabla^2 v + Pr(T - R_\rho S), \quad (5.5c)$$

$$\frac{\partial T}{\partial t} + u \frac{\partial T}{\partial x} + v \frac{\partial T}{\partial y} = \frac{1}{\sqrt{R_T}} \nabla^2 T, \quad (5.5d)$$

$$\frac{\partial S}{\partial t} + u \frac{\partial S}{\partial x} + v \frac{\partial S}{\partial y} = \frac{1}{Le\sqrt{R_T}} \nabla^2 S. \quad (5.5e)$$

In the present calculation, the dimensionless numbers are set as $R_S = 6 \times 10^4$, $R_T = 12 \times 10^4$, and $Pr = 7$; hence $R_\rho = 0.5$. The aspect ratio Ar , which is defined as the ratio of the height to the width of the rectangle, is $Ar = 2$. Two cases with Lewis number given by $Le = 10$, and 100 are simulated. The boundary conditions for the calculations are

$$u = v = 0, \quad \text{on } x = 0, 1 \quad \text{and} \quad y = 0, Ar, \quad (5.6a)$$

$$T = S = -0.5, \quad \text{on } x = 0, \quad (5.6b)$$

$$T = S = 0.5, \quad \text{on } x = 1, \quad (5.6c)$$

$$\frac{\partial T}{\partial y} = \frac{\partial S}{\partial y} = 0, \quad \text{on } y = 0, Ar. \quad (5.6d)$$

The present FDLBM/2 is formulated to recover the set of Eqs. (5.5a)-(5.5e). A steady state solution calculated by the present FDLBM/2 is plotted in Figs. 5 and 6. As Le increases, a thinner solutal boundary layer is observed in the contour plots (cf. Figs. 5(b) and 6(b)).

The numerical results are compared using a mean Nusselt number \overline{Nu} and a mean Sherwood number \overline{Sh} which are defined as

$$\overline{Nu} = \frac{1}{Ar} \int_0^{Ar} \left. \frac{\partial T}{\partial x} \right|_{x=0} dy, \quad \overline{Sh} = \frac{1}{Ar} \int_0^{Ar} \left. \frac{\partial S}{\partial x} \right|_{x=0} dy. \quad (5.7)$$

The Nusselt and Sherwood numbers as calculated by the present FDLBM/2 scheme are listed in Table 1. For larger Le , which means that thermal diffusivity dominates over the diffusivity of concentration, both numbers increase and the increase of \overline{Sh} is more significant. Also, it is shown in Table 1 that both \overline{Nu} and \overline{Sh} are slightly higher for the case with pure thermal convection ($R_\rho = 0$) than for the case where $R_\rho = 0.5$.

Table 1: Mean Nusselt and Sherwood number for different Le and R_ρ at $R_S = 6 \times 10^4$.

\overline{Nu}			\overline{Sh}		
R_ρ	Le		R_ρ	Le	
	10	100		10	100
0	4.7285	4.7285	0	12.42	25.33
0.5	4.5082	4.6591	0.5	10.33	23.27

For the case of pure thermal convection ($R_\rho = 0$), Bejan [38] proposed a theoretically-derived expression for \overline{Nu} for cavities with high Ar . The expression proposed is

$$\overline{Nu} = 0.364 \left(\frac{R_T}{Ar} \right)^{\frac{1}{4}}, \quad (5.8)$$

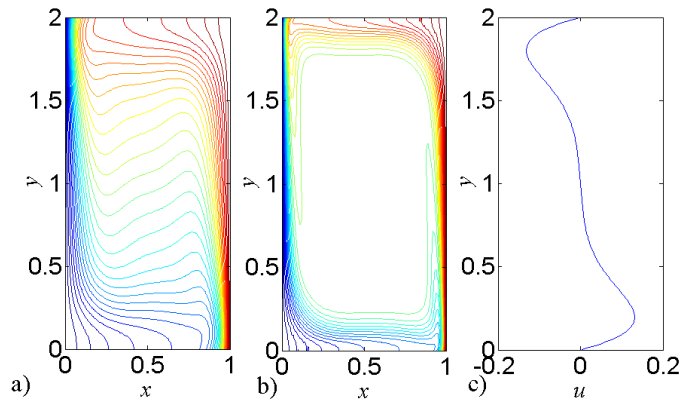


Figure 5: Contour plot of a) temperature, b) salinity, and c) vertical profile of horizontal velocity at $x=0.5$ for $Le=10$, $R_S=6 \times 10^4$, $R_T=12 \times 10^4$, (i.e., $R_\rho=0.5$), $Pr=7$, and $Ar=2$. The numerical parameters are: $\Delta x=0.01$, $\Delta t=0.0001$. There are 30 contour lines with values divided uniformly between maximum value (0.5) and minimum value (-0.5) for each contour plot.

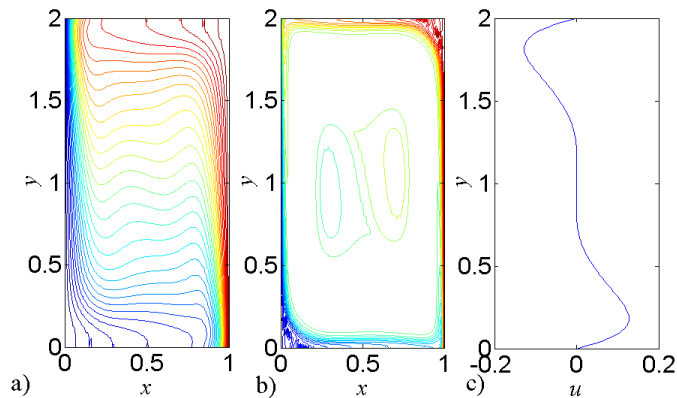


Figure 6: Contour plot of a) temperature, b) salinity, and c) vertical profile of horizontal velocity at $x=0.5$ for $Le=100$, $R_S=6 \times 10^4$, $R_T=12 \times 10^4$, (i.e., $R_\rho=0.5$), $Pr=7$, and $Ar=2$. The numerical parameters are: $\Delta x=0.01$, $\Delta t=0.0001$. There are 30 contour lines with values divided uniformly between maximum value (0.5) and minimum value (-0.5) for each contour plot.

which is suitable for the case when $R_T^{1/7} Ar \rightarrow \infty$. Although the values of $R_T^{1/7} Ar$ for the present case and those reported in [37] are finite, a comparison with the results of Bejan [38] and Lee and Hyun [37] can be attempted for the sake of reference. Table 2 shows the results of \overline{Nu} in different cases. As mentioned before, a quantitative comparison of the FDLBM/2 calculations with the numerical results of [37] cannot be made in this study. However, a consistent trend of \overline{Nu} can be observed in Table 2; thus, the validity of the FDLBM/2 for double diffusive studies is assured. A more detailed calculation will be carried out for quantitative comparison in a later study.

Table 2: Comparison of mean Nusselt number with different R_ρ and R_S .

R_S	R_ρ	Numerical \widetilde{Nu}	Theoretical \widetilde{Nu} [38]	$R_T^{1/7} Ar$
6×10^7 [37]	0	29.10	32.04	28.52
	0.5	28.79		
6×10^4 (FDLBM/2)	0	4.73	5.70	10.63
	0.5	4.66		

6 Conclusions

A discrete flux scheme (DFS) is developed to derive the governing transport equations for two distribution functions; one for mass and another for the thermal energy. It is equivalent to solving the BGK-type modeled LBE that can recover the continuum NS equations fully but is equally valid for gas and liquid flows. For aerodynamic flows, it can be shown that the DFS approach is similar to the lattice Boltzmann equation (LBE) with a BGK-type model and a specified equation of state. Thus formulated, the validity and extent of the DFS have been demonstrated for a variety of aerodynamic and hydrodynamic flow problems including aeroacoustic propagation and scattering by an obstacle, shock capturing, thermal thin film flow along an incline, natural convection in a square and a cubic cavity, and other types of thermal fluid flows. In the present study, two more numerical simulations are reported; one on shock structure and another on double diffusive phenomenon in a rectangular cavity. These simulations are carried out to further demonstrate the validity and extent of the FDLBM/2, which is derived from the DFS, for shock structure simulation, and for double diffusive phenomenon where temperature and salinity gradients are present.

Acknowledgments

S. C. Fu gratefully acknowledges funding support in the form of a PhD studentship awarded him by the Hong Kong Polytechnic University. R. M. C. So acknowledges support received as Co-PI from the NSF Grant CBET-0854411 awarded to New Mexico State University.

References

- [1] P. L. Bhatnagar, E. P. Gross, and M. Krook, A model for collision processes in gases, I. small amplitude processes in charged and neutral one-component systems, *Phys. Rev.*, 94(3) (1954), 511–525.
- [2] D. O. Martinez, W. H. Matthaeus, S. Chen, and D. C. Montgomery, Comparison of spectral method and lattice Boltzmann simulations of two-dimensional hydrodynamics, *Phys. Fluids.*, 6 (1994), 1285–1298.

- [3] S. Chen, and G. D. Doolen, Lattice Boltzmann method for fluid flows, *Annu. Rev. Fluid. Mech.*, 30 (1998), 329–364.
- [4] R. Mei, W. Shyy, D. Yu, and L. S. Luo, Lattice Boltzmann method for 3-D flows with curved boundary, *J. Comput. Phys.*, 161 (2000), 680–699.
- [5] S. C. Fu, W. W. Leung, and R. M. C. So, A lattice Boltzmann based numerical scheme for microchannel flows, *J. Fluids. Eng.*, 131 (2009), 081401.
- [6] G. McNamara, and B. Alder, Analysis of the lattice Boltzmann treatment of hydrodynamics, *Phys. A.*, 194 (1993), 218–228.
- [7] X. He, S. Chen, and G. D. Doolen, A novel thermal model for the lattice Boltzmann method in incompressible limit, *J. Comput. Phys.*, 146 (1998), 282–300.
- [8] X. M. Li, R. C. K. Leung, and R. M. C. So, One-step aeroacoustics simulation using lattice Boltzmann method, *AIAA J.*, 44(1) (2006), 78–89.
- [9] S. C. Fu, R. M. C. So, and R. C. K. Leung, Modeled Boltzmann equation and its application to direct aeroacoustics simulation, *AIAA J.*, 46(7) (2008), 1651–1662.
- [10] E. W. S. Kam, R. M. C. So, and R. C. K. Leung, Acoustic scattering by a localized thermal disturbance, *AIAA J.*, 47(9) (2009), 2039–2052.
- [11] E. W. S. Kam, R. M. C. So, S. C. Fu, and R. C. K. Leung, Finite difference lattice Boltzmann method applied to acoustic-scattering problems, *AIAA J.*, 48(2) (2010), 354–371.
- [12] R. M. C. So, R. C. K. Leung, and S. C. Fu, Modeled Boltzmann equation and its application to shock capturing simulation, *AIAA J.*, 46(12) (2008), 3038–3048.
- [13] R. M. C. So, S. C. Fu, and R. C. K. Leung, Finite difference lattice Boltzmann method for compressible thermal fluids, *AIAA J.*, 48(6) (2010), 1059–1071.
- [14] J. S. Rowlinson, and B. Widom, *Molecular Theory of Capillarity*, Clarendon Press, 1982.
- [15] X. Shan, and H. Chen, Lattice Boltzmann model for simulating flows with multiple phases and components, *Phys. Rev. E.*, 47 (1993), 1815–1820.
- [16] X. Shan, and H. Chen, Simulation of nonideal gases and liquid-gas phase transitions by the lattice Boltzmann equation, *Phys. Rev. E.*, 49 (1994), 2941–2948.
- [17] M. R. Swift, W. R. Osborn, and J. M. Yeomans, Lattice Boltzmann simulation of nonideal fluids, *Phys. Rev. Lett.*, 75 (1995), 830–834.
- [18] J. Chin, E. S. Boek, and P. V. Coveney, Lattice Boltzmann simulation of the flow of binary immiscible fluids with different viscosities using the Shan-Chen microscopic interaction model, *Phil. Trans. Royal. Soc. London. A.*, 360 (2002), 547–558.
- [19] X. Shan, X. F. Yuan, and H. Chen, Kinetic theory representation of hydrodynamics: a way beyond the Navier-Stokes equation, *J. Fluid. Mech.*, 550 (2006), 413–441.
- [20] O. M. Phillips, On flows induced by diffusion in a stably stratified fluid, *Deep. Sea. Res.*, 17 (1970), 435–443.
- [21] C. F. Chen, Double-diffusive convection in an inclined slot, *J. Fluid. Mech.*, 72 (1975), 721–729.
- [22] H. J. S. Fernando, The formation of a layered structure when a stable salinity gradient is heated from below, *J. Fluid. Mech.*, 182 (1987), 525–541.
- [23] X. He, and L. S. Luo, Lattice Boltzmann model for the incompressible Navier-Stokes equation, *J. Stat. Phys.*, 88 (1997), 927–944.
- [24] R. L. Panton, *Incompressible Flow*, 2nd ed., Chapter 10, Wiley-Interscience, New York, 1996.
- [25] S. C. Fu, and R. M. C. So, Modeled lattice Boltzmann equation and the constant density assumption, *AIAA J.*, 47(12) (2009), 3038–3042.
- [26] Z. Guo, B. Shi, and C. Zheng, A coupled lattice BGK model for the Boussinesq equations, *Int. J. Numer. Methods. Fluids.*, 39 (2002), 325–342.

- [27] Q. Li, Y. L. He, Y. Wang, and W. Q. Tao, Coupled double-distribution-function lattice Boltzmann method for the compressible Navier-Stokes equations, *Phys. Rev. E.*, 76 (2007), 056705.
- [28] S. C. Fu, Numerical simulation of blood flow in stenotic arteries, PhD Thesis, Mechanical Engineering Department, Hong Kong Polytechnic University, Hong Kong, 2011.
- [29] E. F. Toro, *Riemann Solvers and Numerical Methods for Fluid Dynamics: A Practical Introduction*, 2nd ed., Chapter 15, Springer-Verlag Berlin Heidelberg, New York, 1999.
- [30] R. Mittal, and G. Iaccarino, Immersed boundary methods, *Annu. Rev. Fluid. Mech.*, 37 (2005), 239–261.
- [31] S. V. Patankar, and D. B. Spalding, A calculation procedure for heat, mass and momentum transfer in three-dimensional parabolic flows, *Int. J. Heat. Mass. Trans.*, 15 (1972), 1787–1806.
- [32] L. H. Kantha, and C. A. Clayson, *Small Scale Processes in Geophysical Fluid Flows*, Academic Press, 2000.
- [33] H. Brenner, Kinematics of volume transport, *Phys. A.*, 349 (2005), 11–59.
- [34] H. Brenner, Navier-Stokes revisited, *Phys. A.*, 349 (2005), 60–132.
- [35] C. J. Greenshields, and J. M. Reese, The structure of shock waves as a test of Brenner's modifications to the Navier-Stokes equations, *J. Fluid. Mech.*, 580 (2007), 407–429.
- [36] H. Alsmeyer, Density profiles in Argon and Nitrogen shock waves measured by the absorption of an electron beam, *J. Fluid. Mech.*, 74 (1976), 497–513.
- [37] J. W. Lee, and J. M. Hyun, Double-diffusive convection in a rectangle with opposing horizontal temperature and concentration gradients, *Int. J. Heat. Mass. Trans.*, 33(8) (1990), 1619–1632.
- [38] A. Bejan, A note on Gill's solution for free convection in a vertical enclosure, *J. Fluid. Mech.*, 90 (1979), 561–568.